Am J Transl Res 2023;15(4):2676-2689
www.ajtr.org /ISSN:1943-8141/AJTR0145573

Original Article

CXCL5 knockdown attenuated gemcitabine resistance of pancreatic cancer through regulation of cancer cells and tumour stroma

Nien-Hung Lee[1], Yi Ma[1], Ching-Seng Ang[2], Chelsea Dumesny[1], Nhi Huynh[1,3], Yang Yang[1], Kai Wang[1], Mehrdad Nikfarjam[1], Hong He[1]

[1]Department of Surgery, University of Melbourne, Austin Health, Heidelberg, Victoria, Australia; [2]Bio-21 Institute, University of Melbourne, Parkville, Victoria, Australia; [3]Tumour Targeting Laboratory, Level 5, ONJCRI, Heidelberg, Victoria, Australia

Received July 26, 2022; Accepted December 28, 2022; Epub April 15, 2023; Published April 30, 2023

Abstract: Chemoresistance is one of the major causes to the poor prognosis of pancreatic cancer (PC). Gemcitabine alone and gemcitabine-based therapies are mostly used for the treatment of PC. Gemcitabine resistance becomes the focus of chemotherapy. C-X-C motif chemokine 5 (CXCL5), a member of the C-X-C chemokine family, acts through C-X-C chemokine receptor type 2 (CXCR2). A high level of CXCL5 is associated with worse prognosis in PC patients and increased suppressive immune cell infiltration. Increased expression of CXCL5 is also found in gemcitabine-treated PC cells. To investigate the role of CXCL5 in PC response to gemcitabine, CXCL5 knockdown (KD) PC cells were generated and its effect on cancer cell response to gemcitabine *in vitro* and *in vivo* was studied. The mechanisms involved were also explored by determining the changes in the tumour microenvironment (TME) and protein profile of the CXCL5 KD cells using immune-staining and proteomic analysis. The results showed that CXCL5 expression were increased in all PC cell lines tested and in gemcitabine-resistant tumour tissue, that CXCL5 KD suppressed PC growth and sensitized PC cell response to gemcitabine and that CXCL5 KD stimulated the activation of stromal cells in TME. We conclude that CXCL5 promotes gemcitabine resistance by affecting TME and cancer cells.

Keywords: CXL5, CXCR2, gemcitabine, α-SMA, collagen I, tumour stroma

Introduction

Over 80% of pancreatic cancer (PC) patients present with advanced stage of cancer at diagnosis [1], which leaves them with only palliative treatment (mainly chemotherapy) options, with a median survival less than 1 year, regardless of the use of various therapy regimens [2, 3]. Chemoresistance becomes one of the major contributors to the poor prognosis of PC with a 5-year survival rate of less than 10% [4]. The unique tumour stroma/microenvironment (TME) characterized by pronounced desmoplasia in PC plays a key role in chemoresistance. Type I collagen (Col1) is a major component of the TME [5, 6]. Activated pancreatic stellate cells (PSCs) express high levels of alpha-Smooth muscle actin (α-SMA) and contribute significantly to the production of Col1. Col1 composes of the major structure of PC stroma which is proposed to reduce drug delivery to cancer cells and restrict T-cell infiltration [7-10]. Modulation of TME to overcome chemoresistance becomes a focus in PC research.

Gemcitabine and gemcitabine-based combination therapies, such as gemcitabine plus Nab-paclitaxel, have been mostly used for the treatment of PC in all stages of the disease. Thus, the resistance to gemcitabine has been extensively studied to find a way to overcome its resistance to improve the outcome of treatment. Gemcitabine resistance has been clarified into two types, intrinsic to cancer cells and extrinsic from TME. When activated by cancer cells, PSCs, one of the main components of tumour stroma, secret extracellular matrix (ECM) proteins, including collagen, fibronectin, and laminin to form a dense matrix around cancer cells. PSCs stimulate Hes1 expression of

cancer cells through the Notch signalling pathway, enhancing chemoresistance to gemcitabine [11]. PSCs also promote gemcitabine resistance by paracrine SDF-1α/CXCR4 signalling-activated intracellular FAK-AKT and ERK1/2 signalling pathways and subsequent IL-6 autocrine loop in cancer cells [12].

C-X-C motif chemokine 5 (CXCL5), a member of the C-X-C chemokine family, acts through C-X-C chemokine receptor type 2 (CXCR2) and affects many cellular functions including neutrophil trafficking, tumour cell migration/invasion [13, 14]. PC cell secrets CXCL5 which in turn stimulates cancer cell migration/invasion [15]. CXCL5 from the cell-conditioned media of PC cell lines induces angiogenesis through binding to CXCR2 [16]. CXCL5 also stimulates the proliferation of PC cell lines via CXCR2 receptor [17]. CXCL5 is over-expressed in PC tissues. High CXCL5 expression is associated with worse prognosis of PC patients and increased suppressive immune cell infiltration [18]. Gemcitabine-treated PC cell lines showed a higher level of CXCL5 compared to non-treated cells [19]. An antagonist of CXCR2 reduced the resistance of PC cells to gemcitabine. However, the direct effect of CXCL5 on gemcitabine resistance hasn't been investigated.

In this study, we have investigated the role of CXCL5 in the inhibitory effect of gemcitabine on PC using cell-based assays and mouse experiments. We have generated CXCL5 knockdown PC cell lines and determined the gemcitabine effect in comparison with control cells *in vitro* and *in vivo*. We have also explored the mechanism(s) involved by measuring the effect of CXCL5 knockdown on TME using immunohistochemical staining and proteomic analysis.

Materials and methods

Cell culture and reagents

Human PC cell lines, AsPC-1, BxPC3, Capan-2, CFPAC-1, HPAF-2, MiaPaCa-2, Panc-1, PL45 and SW1999 were purchased from American Type Culture Collection (ATCC, Manassas, VA) and cultured in Dulbecco's modified Eagle's medium (DMEM) (Sigma-Aldrich, MO) with 5% fetal bovine serum (FBS) (HyClone, UT) in humidified air with 5% CO_2 at 37°C. A human pancreatic duct epithelial (HDPE) cell line was obtained from TS Tsao (Ontario Cancer Institute, Ontario, Canada). All cell lines were tested negative for mycoplasma. 5-Fluorouracil powder (5-FU) with purity ≥ 99% (HPLC), was purchased from Sigma (5-FU; F6627, Sigma-Aldrich Inc., St. Louis, MO, USA). Gemcitabine from Hospira (AUST R 160204, Hospira Pty Ltd., Melbourne, Victoria, Australia). Anti-Cleaved Caspase 3 antibody (#9661) was provided by Cell Signaling Technology Inc. (Danvers, MA, USA). Anti-CXCL5 antibody (ab9802) and anti-CXCL10 antibody (ab9807) were from Abcam (Cambridge, United Kingdom). Anti-Ki67 antibody (RM9106S) from Thermo-Fisher Scientific Corp. (Grand Island, NY, USA), α-SMA antibody (ab32575) from Abcam (Melbourne, Australia) and Fibronectin antibody (15613-1-AP) from Proteintech (United States).

Determination of mRNA levels of CXCLs by reverse transcription polymerase chain reaction (RT-PCR)

A panel of human PC cells as well as a normal human pancreatic ductal epithelial cell (HDPE) were grown in 6-cm culture dishes containing DMEM (5% FBS) to 80-90% confluency. Total RNAs were extracted using TRIzol reagent (Invitrogen, Thermo-Fisher Scientific, CA). 4 μg RNA of each sample was mixed with RNase inhibitor (Promega, WI), dNTP mixture (Takara Bio, Shiga, Japan) and 20 μl Oligo-dT (MDBio, Shandong, China) in reverse transcription buffer (Promega, WI). After heating at 70°C to remove any secondary structure in total RNA samples, reverse transcriptase (Promega, WI) (2 μl/tube) was added to start reverse transcription at 42°C and the reaction was maintained for 65 min to generate cDNA samples which were heated at 90°C for 5 min to inactivate reverse transcriptase and cooled down at 4°C for 99 min.

For PCR, 5 μl 10 × Standard Reaction Buffer (Takara Bio, Shiga, Japan), 28 μl dNTP mixture, 14 μl 10 μM forward primer (Supplementary Table 1) solution, 14 μl 10 μM reverse primer (Supplementary Table 1) solution and 3.5 μl Taq polymerase (Takara Bio, Shiga, Japan) were mixed in a 1.5 ml microcentrifuge tube to generate PCR reagent mixtures. A 5 μl cDNA sample was added to a PCR tube containing 13.5 μl of PCR reagent mixture and amplified in 20-35 cycles of reaction. The resultant PCR products were run in a 2% agarose gel in 0.5 × TAE buffer. The DNA bands were visualized with GelRed

Nucleic Acid Gel Stain (Biotium, CA) and the densities of the bands were analyzed using Quantity One 1-D Analysis Software (Version 4.6.9, Bio-Rad Laboratories, CA).

Generating CXCL5 knockdown cells

To obtain CXCL5 knockdown (KD) cells, MiaPaCa-2 cells were transfected with plasmid DNAs encoding shRNA sequences (OriGene Technologies, MD) to silence the CXCL5 gene specifically or with a scrambled sequence (OriGene Technologies, MD) as a negative control using Lipofectamine Reagent (Invitrogen, Melbourne, Australia) according to the manufacturer's instructions. Stable clones were selected with puromycin (0.5 μg/ml). CXCL5 mRNA expression was determined by RT-PCR.

Cell proliferation assay

Both negative control (NC, cells transfected with a scrambled sequence) and CXCL5 knockdown (KD) MiaPaCa-2 cells were incubated with gemcitabine or 5-FU with concentrations indicated in the result section for 48 h. Cell proliferation was determined by MTT assay and the IC50 values for the inhibitory effects of gemcitabine and 5-FU were calculated from three sets of independent experiments.

Mouse study

The mouse experiments were approved by the Austin Health Animal Ethics Committee (A2018/05509). Experimental mice were housed at controlled constant temperatures and humidity with alternating 12-hour long cycles of light and dark in the BioResource Facility at Austin Health and monitored according to health criteria. Both NC and CXCL5 KD human PC cells MiaPaCa-2 (5×10^6 cells/100 μl culture medium) were subcutaneously injected into the flanks of 6-week-old, male Scid mice. When a clear tumour size can be measured between 20 and 50 mm^3, gemcitabine (50 mg/Kg) was given by intraperitoneal injection twice a week. The control mice were given the same volume of saline. Tumour growth was determined by tumour volume measured by a calliper every other day and by tumour weight determined at the end of the experiment. The interaction between CXCL5 KD and gemcitabine was calculated using the Coefficient of Drug Interaction (CDI) index according to the equation [20]: CDI=R12/(R1 × R2) where R12 represents a tumour volume in combined treatment, and R1 and R2 tumour volumes in every single treatment.

Sirius red and immunohistochemical staining

Paraffin-embedded xenografted tumour tissues were sectioned into 5 μM slides with LEICA RM2245 microtome (Leica Biosystems, Germany). For Sirius red staining, tissue slides were incubated in Sirius red (0.1% Sirius red in saturated picric acid solution) for 1 hour and then rinsed twice in acidified water containing 0.5% acetic acid. After rehydration, the slides were mounted with DPX mounting medium (VWR International Ltd., United Kingdom) and left to dry for 24 hours before analysis.

For Immunohistochemistry (IHC), after dewaxing, antigens were retrieved by boiling tissue slides in 10 mM citrate buffer (pH 6.0) for 30 min in a 99°C water bath, followed by cooling at room temperature for 20 min. Endogenous peroxidase quenching was achieved by incubating slides in Dako REAL™ peroxidase blocking solution (Agilent Technologies, Denmark) for 15 min in dark. The slides were blocked for non-specific binding in 5% normal goat serum (NGS) plus 1% bovine serum albumin (BSA) in TBS-T for an hour at room temperature, and then incubated overnight at 4°C with primary antibodies of interest, which includes Caspase 3 antibody (1:500 dilution, Cell Signaling Technology Inc., Danvers, MA, USA), CXCL5 antibody (1:500 dilution, Abcam PLC, Cambridge, United Kingdom), CXCL10 antibody (1:2000 dilution, Abcam PLC, Cambridge, United Kingdom), Ki67 antibody (1:1000 dilution, Thermo-Fisher Scientific Corp., Grand Island, NY, USA), α-SMA antibody (1:500 dilution in 1% BSA in TBST, Abcam, Australia) and Fibronectin antibody (1:200 dilution in 1% BSA in TBST, Proteintech, USA) respectively. For secondary antibody, the slides were incubated with HRP labelled polymer anti-rabbit antibody (Agilent technologies, Denmark) for an hour. They were then stained with EnVision FLEX DAB plus Substrate Chromogen System (Dako Omnis, Agilent technologies, Denmark) and counterstained with Haematoxylin. The slides were then rehydrated and mounted with DPX mounting medium (VWR International Ltd., United Kingdom) and left to dry for 24 hours before analysis.

Images of each sample were captured with a LEICA DM4000B microscope (Leica Biosystems, Germany). For both Sirius red staining and IHC of α-SMA and Fibronectin, the Fiji image analysis platform [21] was used, and the positively stained area was measured and calculated as a percentage of the total area of the sample. The images obtained from IHC of Ki67, Caspase 3, CXCL5 and CXCL10, were analysed using Image-Pro Plus (Version 4.5.0.29, Media Cybernetics Inc., Maryland, USA). A constant intensity threshold was used for each analysis to ensure the same definition of staining positivity across different samples.

Proteomic analysis

NC and CXCL5 KD MiaPaCa-2 (1×10^6 cells) were seeded in a 10 cm culture dish and grown to < 80% of confluency when the cells were lysed with radioimmunoprecipitation assay (RIPA) buffer (25 mM Tris HCl, pH 8, 150 mM NaCl, 1% Triton x-100, 1% Na deoxycholate, 0.5% SDS, 1 mM EGTA, protease inhibitor, pHos sTop). The supernatant was precipitated with ice-cold acetone overnight at -20°C before resuspension in 8 M urea (in 50 mM triethylammonium bicarbonate + 10 mM TCEP) followed by incubation at 37°C for 30 mins. Protein concentration was quantified using a BCA protein assay. Samples were diluted to a final concentration of 1 M urea followed by overnight digestion at 37°C with sequencing-grade modified trypsin (Thermofisher) at a ratio of 1:50 (enzyme:protein). Digestion was stopped by the addition of formic acid to a final concentration of 1% (v/v). The peptide mix was purified through a solid phase extraction (SPE) with Oasis HLB cartridges (Waters) according to the manufacturer's instructions. Eluted peptides were resuspended in 2% acetonitrile and 0.05% trifluoroacetic acid for global mass spectroscopy. The data obtained from mass spectroscopy were processed through MaxQuant (version 1.6.17.0) [22] and searched against the Homo Sapiens database (SwissProt Taxonomy ID 9606, updated Dec 2020). The search parameters are Trypsin as the cleavage enzyme and a maximum of 2 missed cleavages. Instrument parameters are based on the default Maxquant setup. Carbamidomethyl cysteine was set as a fixed modification. The LFQ algorithm was used for label-free quantitation and a match between runs was activated. Protein and peptides groups were set to a maximum false discovery rate (FDR) of < 0.01. Statistical and network analysis of the search results was carried out before using Perseus software (version 1.6.14.0) [23] and Cytoscape (version 3.8.2) [24].

Statistical analysis

Mean and standard error are used to express all values. Data obtained from tumour tissues were collated according to the number of tumour samples. Data were analysed by one-way ANOVA or t-test (SPSS, IBM, New York, NY). Differences between the two means with $P < 0.05$ were considered significant.

Results

CXCL5 level increased in PC cell lines and chemoresistant pancreatic tumour tissues

The mRNA levels of six members of CXCL chemokines were determined in a panel of nine human pancreatic cancer (PC) cell lines compared with the normal pancreatic epithelial cells (HDPE). Among the six CXCLs (CXCL1, 2, 5, 9, 10, 13), CXCL5 expression was increased in all nine PC cell lines shown in **Figure 1A**, compared to normal pancreatic cell, HDPE. The levels of the other 5 CXCLs varied among the nine PC cell lines. The level of CXCL10 was decreased in seven PC cell lines compared to normal pancreatic epithelial cells (**Figure 1A**) while the CXCL9 level was similar in all cell lines examined including normal pancreatic epithelial cells. Thus the protein expressions of CXCL5 and CXCL10 were determined in xenografted tumour tissues treated with gemcitabine plus or minus Nab-paclitaxel or PF-3758309 (an inhibitor of pan p21 activated kinases), obtained from our previous study [25]. The CXCL5 protein levels were increased to 400%, 300% and 395% of non-treated control tumours (**Figure 1B**, **1C**). The protein expression of CXCL10 was not significantly changed (**Figure 1B**, **1D**). These results indicate a role of CXCL5 in chemoresistance, such as gemcitabine resistance of PC.

Knockdown of CXCL5 sensitized pancreatic cancer cell response to gemcitabine

To determine the effect of CXCL5 on PC response to gemcitabine, CXCL5 knockdown

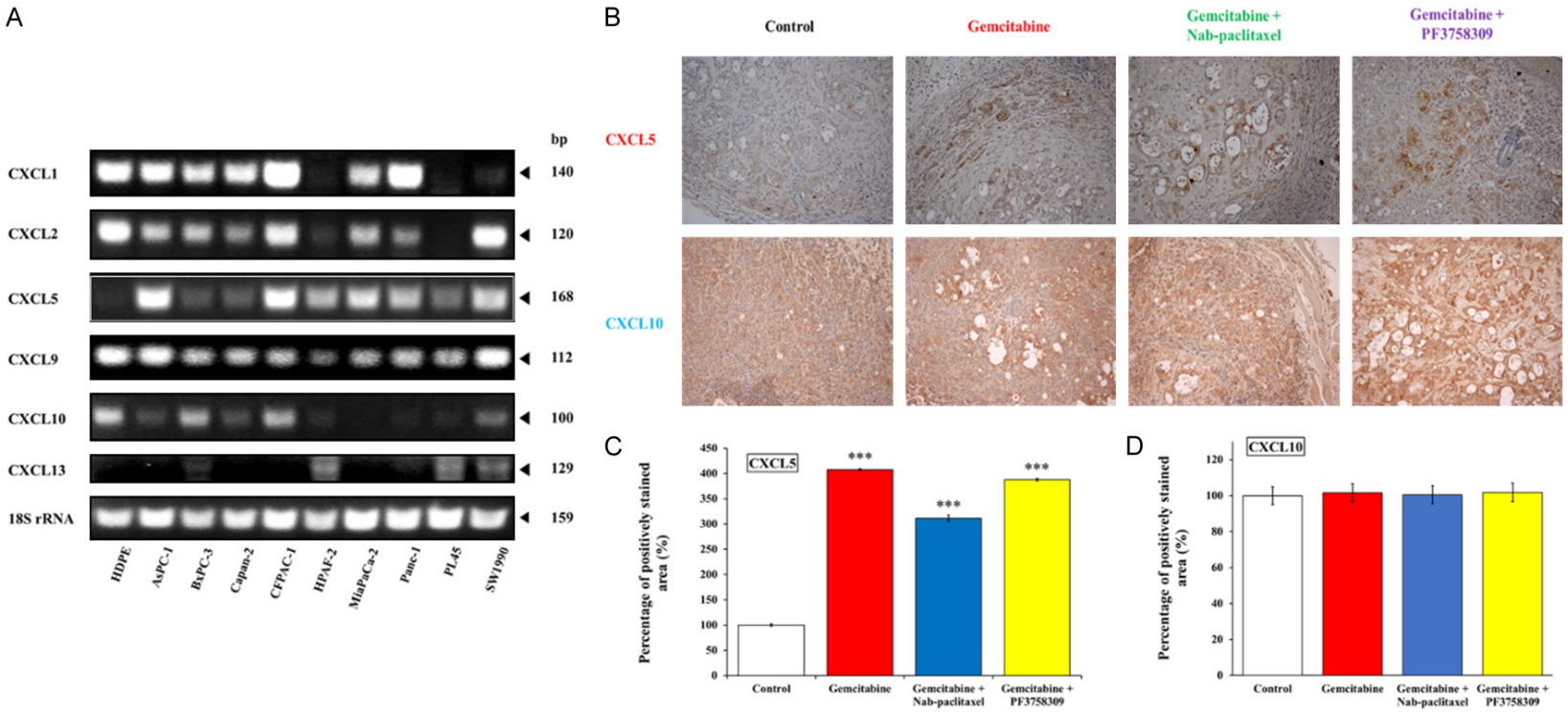

Figure 1. CXCL5 is overexpressed in pancreatic cancer cells and tumour tissues treated with multiple chemo reagents. The mRNA levels of CXCL1, 2, 5, 9, 10 and 13 in a panel of human pancreatic cells as well as normal pancreatic epithelial cells (HDPE) were determined by reverse transcriptive PCR as described in the Materials and Methods. The mRNA expression of CXCL5 was elevated in all pancreatic cell lines tested compared to the normal pancreatic epithelial cells (HDPE) as shown in (A). The mRNA of CXCL10 was decreased in seven out of nine cell lines tested (A) and the remaining two lines had similar levels of CXCL10 to HDPE cells. The protein levels of CXCL5 and 10 in xenografted pancreatic tumours (6 samples in each group) were determined by immunohistochemical staining. Compared to the control, the protein levels of CXCL5 were increased in tumours treated with gemcitabine plus or minus Nab-paclitaxel or PF3758309 (B and C) while the protein levels of CXCL10 had no significant changes (B and D). ***, $P < 0.001$ compared to control.

(KD) MiaPaCa-2 cells were generated using shRNA. The level of mRNA expression was determined by RT-PCR, and two clones with low CXCL5 expression (**Figure 2A**) were selected for cell proliferation assay. Knockdown of CXCL5 sensitized PC cell response to the treatment of gemcitabine and 5-FU, and the IC50 values of gemcitabine and 5-FU calculated from cell proliferation assays were significantly lower as shown in **Figure 2B**. Furthermore, the effect of CXCL5 knockdown on PC growth with or without gemcitabine treatment was tested in a Scid mouse xenografted model as described in the Materials and Methods. CXCL5 knockdown reduced pancreatic tumour growth on its own by decreasing tumour volume maximally to 11.68% of control (**Figure 2D**), and by reducing tumour weight to 16.38% of control (**Figure 2E**). CXCL-5 knockdown also enhanced the inhibitory effect of gemcitabine on these tumour growths shown by further reduced tumour volume (**Figure 2D**) to 50.95% of gemcitabine-treated NC (negative control cell transfected with a scramble sequence) tumour and tumour weight (**Figure 2E**) to 11.57% of gemcitabine-treated NC tumour. The interaction between gemcitabine and CXCL5 *in vivo* was calculated using the Coefficient of Drug Interaction (CDI) method, and CXCL5 KD synergistically stimulated the inhibitory effect of gemcitabine on pancreatic cancer growth *in vivo* as all CDI values calculated through the period of treatment were less than 1 [20]. These results showed that inhibition of CXCL5 by knockdown suppressed pancreatic tumour growth and sensitized PC cells' response to gemcitabine *in vitro* and *in vivo*, indicating that CXCL5 plays an important role in pancreatic cancer growth and chemoresistance.

Knockdown of CXCL5 enhanced the inhibitory effect of gemcitabine on pancreatic tumours by decreasing proliferation and promoting apoptosis

To investigate the mechanism(s) involved in the effects of CXCL5 knockdown on pancreatic tumours and how CXCL5 knockdown affected the gemcitabine effect, tumour tissues isolated from the experiment described above were immunohistochemically stained with anti-Ki67 and anti-caspase 3 (cleaved active form) antibodies to determine tumour cell proliferation and apoptosis. CXCL-5 protein levels in these tumour tissues were also determined by immunohistochemical (IHC) staining. CXCL5 knockdown inhibited tumour cell proliferation by reducing the numbers of Ki67 stained cells (**Figure 3A** and **3D**) and enhanced apoptosis of tumour cells via increasing the numbers of cleaved active caspase 3 stained cells (**Figure 3B** and **3E**). Similar effects were observed in gemcitabine-treated tumours inoculated by negative control (NC) cells (**Figure 3A**, **3B**, **3D**, **3E**). In tumours inoculated by CXCL5 KD cells, gemcitabine treatment further decreased tumour cell proliferation (**Figure 3A** and **3D**) and increased cell apoptosis (**Figure 3B** and **3E**). Like our findings shown in **Figure 1**, the levels of CXCL5 protein were increased in gemcitabine-treated tumours inoculated by both NC and CXCL5 KD cells. These results indicated that CXCL5 KD suppressed pancreatic tumour growth and enhanced the inhibitory effect of gemcitabine on the pancreatic tumour by decreasing cell proliferation and by promoting cell apoptosis. The increased expression of CXCL5 in tumour tissue treated with gemcitabine further confirmed our findings in **Figure 1**, suggesting a role of CXCL5 in the chemoresistance of pancreatic cancer.

CXCL5 knockdown stimulated Col1 and α-SMA expression in the pancreatic tumour microenvironment

The tumour stroma/microenvironment plays a pivotal role in pancreatic carcinogenesis and chemoresistance. Col1 is a major component of the tumour stroma. α-SMA is a marker of activated pancreatic stellate cells (PSCs) responsible for the formation of a desmoplastic stroma of pancreatic tumour. Fibronectin, a secreted protein in PC stroma, contributes to gemcitabine resistance and poor patients' survival. To determine the role of CXL5 knockdown on tumour stroma of pancreatic cancer, the protein expressions of Col1, α-SMA and fibronectin were measured by IHC stain of tumour tissues isolated from the xenografted tumours in the experiment described above. As shown in **Figure 4**, regardless of gemcitabine treatment, CXCL5 knockdown increased the protein expression of Col1 in tumour tissues treated with or without gemcitabine (**Figure 4A** and **4D**). Likewise, the knockdown of CXCL5 stimulated the protein expression of α-SMA (**Figure 4B** and **4E**). Gemcitabine treatment did not

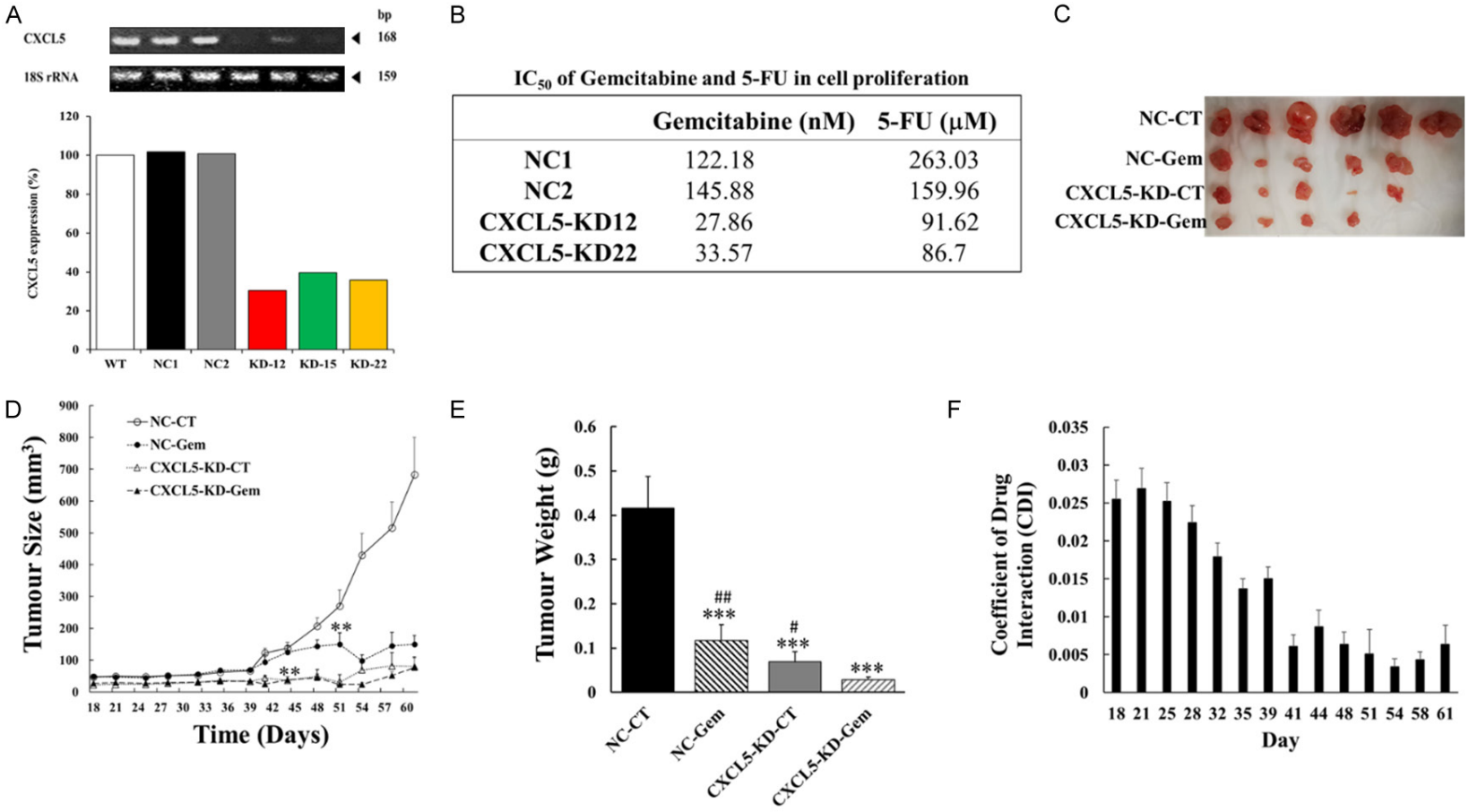

Figure 2. Knockdown of CXCL5 inhibited pancreatic cancer and sensitized cancer cell response to chemo-treatment. Knockdown of CXCL5 clones in MiaPaCa-2 cell line were generated by transfecting cells with shRNA and the clones with a significant reduction in CXCL5 mRNA determined by RT-PCR were shown in (A). Two negative control (NC, transfected with a scramble sequence) clones, NC1 and NC2, and two CXCL5 knockdown (KD) clones (KD-12 and KD-22) were subjected to cell proliferation assay in the presence or absence of gemcitabine (Gem) or 5-FU. CXCL5KD clones showed lower IC50 values of gemcitabine and 5-FU compared to NC cells (B). NC and CXCL5-KD (KD-22) cells were injected into the flanks of a Scid mouse. By day 18 of cell injection when tumour volume can be measured, mice were treated with gemcitabine (50 mg/Kg) twice a week for 6 weeks. 6, 5, 5, and 4 mice were allocated in NC-control (NC-CT), NC-gemcitabine-treated (NC-Gem), CXCL5 KD-control (CXCL5-KD-CT) and CXCL5-KD-Gem respectively. Each tumour image was shown in (C). CXCL5 KD suppressed tumour growth by reducing tumour volume (D) and weight (E). Gemcitabine inhibited NC tumour growth by reducing tumour volume (D) and weight (E). CXCL5 KD enhanced the inhibitory effect of gemcitabine shown by further reduced tumour volume (D) and weight (E) compared to gemcitabine-treated NC tumours. The interaction between Gem and CXCL5 *in vivo* (F) was calculated using the Coefficient of Drug Interaction (CDI) equation as described in the Material and Methods. CT: control; **, $P < 0.01$; ***, $P < 0.001$ compared to NC-CT. #, $P < 0.05$; ##, $P < 0.01$ compared to gemcitabine-treated CXCL5-KD.

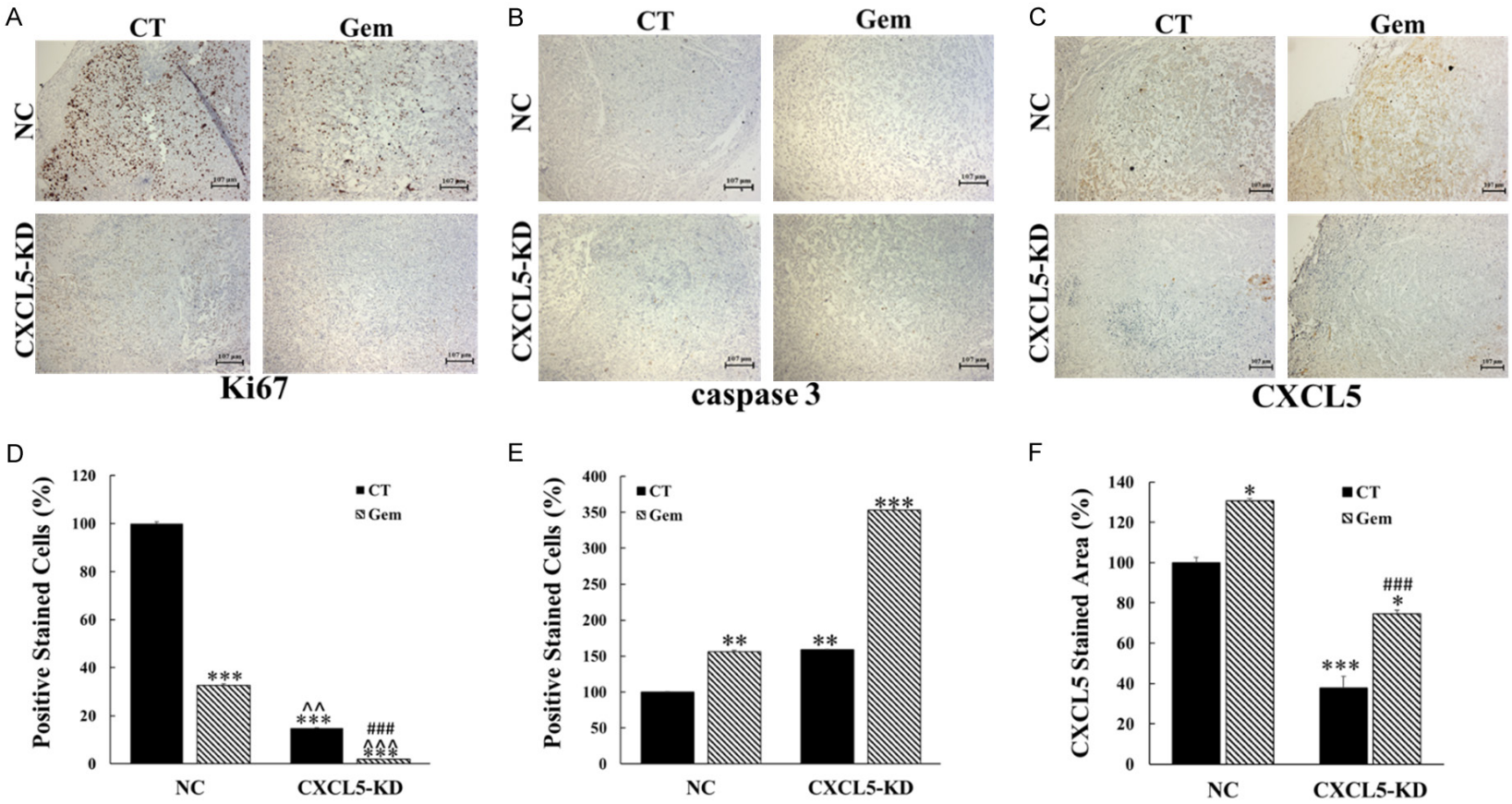

Figure 3. Knockdown CXCL5 enhanced the inhibitory effect of gemcitabine on pancreatic tumours by decreasing proliferation and promoting apoptosis. Tumour tissues obtained from experiments described in **Figure 2** were stained with anti-Ki67 and anti-caspase 3 (cleaved active form) antibodies to determine cell proliferation and apoptosis respectively. CXCL5 knockdown (KD) decreased cell proliferation and enhanced apoptosis by reducing Ki67 stained cells (A and D) and increasing cleaved active caspase 3 stained cells (B and E). Within NC cells, gemcitabine (Gem) treatment decreased cell proliferation and enhanced apoptosis by reducing Ki67 stained cells (A and D) and increasing cleaved active caspase 3 stained cells (B and E). In CXCL5 KD cells, gemcitabine treatment further decreased cell proliferation and stimulated apoptosis by further reducing Ki67 stained cells (A and D) and increasing cleaved active caspase 3 stained cells (B and E). Gemcitabine treatment increased the protein expressions of CXCL5 in both NC and CXCL5 KD cells (C and F). 6, 5, 5 and 4 samples were used for NC-CT, NC-Gem, CXCL5-KD, and CXCL5-KD-Gem respectively. CT: control; NC: negative control cells; *, $P < 0.05$; **, $P < 0.01$; ***, $P < 0.001$; compared to NC-CT; ^^, $P < 0.01$; ^^^, $P < 0.001$; compared to gemcitabine-treated NC; ###, $P < 0.001$; compared to gemcitabine-treated CXCL5-KD.

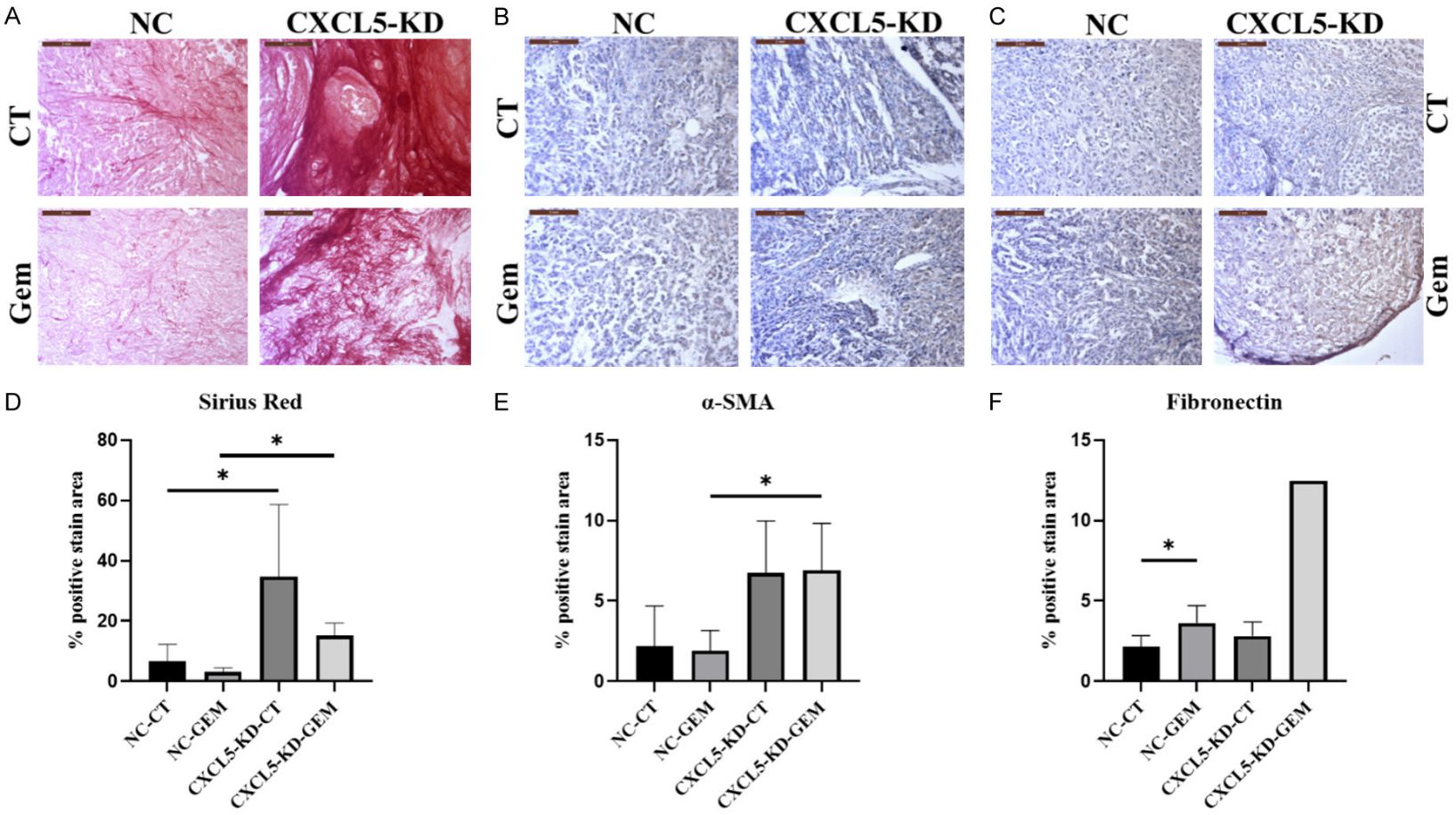

Figure 4. CXCL5 knockdown stimulated collagen I and α-SMA expression in the pancreatic tumour microenvironment. Tumour tissues obtained from experiments described in **Figure 2** were stained with Sirius Red to determine the expression of Col1, and IHC-stained with anti-α-SMA and anti-fibronectin antibodies. The positively stained areas were analysed as described in the Materials and Methods. The expression of Col1 (A and D) as well as α-SMA (B and E) were increased in CXCL5 knockdown tumour tissues regardless of gemcitabine (Gem) treatment. CXCL5 knockdown did not change the expression of fibronectin (C and F) while gemcitabine treatment seemed to increase the expression of fibronectin in both NC- and CXCL5-KD-inoculated tumours (C and F). 6, 4, 3 and 2 samples were used for NC-CT, NC-Gem, CXCL5-KD, and CXCL5-KD-Gem respectively. CT: control; *, $P < 0.05$.

affect either Col1 or α-SMA protein expression in either NC- or CXCL5-KD-inoculated tumours. The protein expression of fibronectin was increased in gemcitabine-treated tumour tissues inoculated by NC cells (**Figure 4C** and **4F**). Gemcitabine also increased fibronectin expression in CXCL5-KD-inoculated tumours. However, there were not enough tumour samples collected in the gemcitabine-treated CXCL5-KD tumor group due to the very small volumes of these tumours (**Figure 2C**). The statistical significance could not be calculated due to the limited numbers of samples used in the analysis. Nevertheless, these results demonstrated a role of CXCL5 in pancreatic TME of pancreatic cancer, which would contribute to the effect of CXCL5 on pancreatic carcinogenesis and chemoresistance.

Molecular changes induced by CXCL5 knockdown

To investigate the molecular mechanism(s) involved in CXCL5 knockdown, the global protein profiles were obtained and compared between NC and CXCL5 KD using proteomic analysis described in the Materials and Methods. Compared to NC cells, the levels of 12 proteins were increased in CXCL5 KD cells (**Figure 5A** and **5B**) while the expressions of 11 proteins were decreased in CXCL5 KD cells. These significant hits (proteins) were input into Cytoscape for the network analysis. 16 out of the total 23 proteins were taken up by the software in the analysis. 4 (FSCN1, DUS3, AASS, and HTRA1) out of 12 up-regulated proteins and 5 (TDRKH, PCBP3, GSTM1, GSTM3 and PTGES) out of 11 down-regulated proteins by CXCL5 knockdown were shown in the identified network (**Figure 5C**). Further analysis from String linked to Cytoscape revealed that some of these proteins with significant changes, were identified in KEGG (Kyoto Encyclopedia of Genes and Genomes) pathways of drug metabolism or other enzymes (**Figure 5D**) and involved in a few GO (Gene Oncology) functions including oxidoreductase activity, iron-sulphur cluster binding, and modified amino acid binding (**Figure 5D**). These data identified the proteins that were significantly up- or down-regulated by CXCL5 knockdown and the possible pathway(s) involved.

Discussion

We have demonstrated in this paper that knockdown of CXCL5 inhibited pancreatic cancer and enhanced the inhibitory effect of gemcitabine on pancreatic cancer, that knockdown of CXCL5 caused the increased levels of Col1 and α-SMA in pancreatic tumour stroma/microenvironment. These results indicated that CXCL5 stimulated pancreatic cancer and contributed to gemcitabine resistance probably through regulation of the tumour stroma/microenvironment.

We have found that the expression of CXCL5 increased not only in all nine PC cell lines tested but also in patient-derived xenografted tumours treated with gemcitabine and other chemo-reagents. Consistent with the previous report that gemcitabine-treated PC cell lines had increased CXCL5 expression, we have shown that treatments by gemcitabine and gemcitabine plus other chemo-reagents of pancreatic tumour tissues caused increased CXCL5 protein expression *in vivo* (**Figure 1B** and **1C**), which linked CXCL5 to chemoresistance of PC. The fact that inhibition of CXCL5 by knockdown using shRNA, sensitized PC cell response to gemcitabine and 5-FU, and that CXCL5 knockdown not only suppressed pancreatic tumour growth on its own but also synergistically enhanced the inhibitory effect of gemcitabine on pancreatic tumour growth (**Figure 2**) by reducing cancer cell proliferation and promoting apoptosis (**Figure 3**), have indicated that CXCL5 mediated gemcitabine resistance in pancreatic cancer.

More interestingly we have found that knockdown of CXCL5 in PC cells increased the protein expression of Col1 and α-SMA in tumour stroma/microenvironment. It has been recognized that the stromal active PSCs/α-SMA$^+$ myofibroblasts stimulate Col1 production contributing to the stiffness of tumour stroma which in turn contributes to chemoresistance of PC [26-30]. It has been recognized that Col1 stimulated PC cell proliferation, promoted malignancy of PC cells and extended cancer cell survival under chemotherapy [27]. However, deletion of Col1 in a mouse model of pancreatic ductal carcinoma (PDA) accelerated the emergence of pancreatic intraepithelial neoplasia (PanIN) and PDA, decreasing overall survival [31]. Col1 deletion led to upregulation of CXCL5. Increased CXCL5 induced recruitment of myeloid-derived suppressor cells and suppression of CD8+ T cells, and this effect of CXCL5 can be attenuated with combined targeting of CXCR2 and CCR2 to restrain accelerated PC progression in

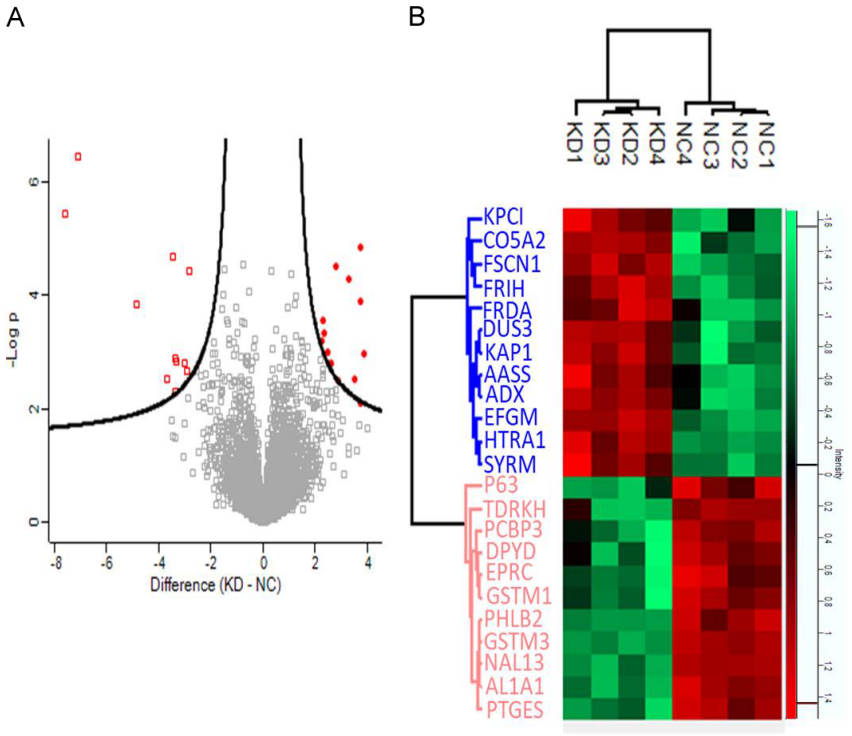

D

Pathway and function analysis

Genes	Category	Description	FDR value	p-value
GSTM3|GSTM1|PTGES	GO Function	Glutathione binding	0.0011	0.000000202
GSTM3|RPE65|GSTM1|PTGES	GO Function	Modified amino acid binding	0.0015	0.000000867
GSTM3|GSTM1|DPYD	KEGG Pathways	Drug metabolism - other enzymes	0.0149	0.0000328
FDX1|RPE65|DUS3L|DPYD|FXN|AASS	GO Function	Oxidoreductase activity	0.0203	0.0000155
FDX1|DPYD|FXN	GO Function	Iron-sulfur cluster binding	0.0237	0.0000227

Figure 5. Molecular changes induced by CXCL5 knockdown. Cell lysates from both negative control (NC, transfected with a scramble sequence) and CXCL5 knockdown (KD, KD-22) were subjected to proteomic analysis as described in the Materials and Methods. A global protein profile was generated. CXCL5 KD increased 12 proteins (solid circles in (A), red-coloured blocks in (B) compared to NC while decreasing 11 proteins (open squares in (A), green-coloured blocks in (B) as demonstrated by the volcano graph (A) and heatmap (B). 4 out of 12 up-regulated proteins and 5 out of 11 down-regulated proteins were identified from a network analysis by Cytoscape software (C). The green-coloured circles represented proteins down-regulated while the red-coloured circles proteins up-regulated. The deeper the colour, the more changes were induced by CXCL5 KD. The grey lines represented the link in a network. The thicker a line, the stronger the link. The results from the pathway and function analysis were listed in (D).

the setting of stromal Col1 deletion. Consistent with these published findings, our data demonstrated that the stromal Col1 was increased in pancreatic tumour inoculated by CXCL5 knockdown PC cells.

Likewise, activated PSCs act through the secretion of extracellular matrix proteins and soluble factors to stimulate PC via multiple signalling pathways [32]. A high level of α-SMA, a marker of activated PSCs is associated with worse overall survival of PC patients [33, 34]. However, simply deleting PSCs paradoxically promoted PC progression in mouse models, indicating a cancer-inhibitory role of PSCs [35, 36]. It has been reported in PC that low α-SMA was related to high nodal involvement, microvascular invasion, low tumour differentiation, and high TNM stage [37] and that α-SMA level was not significantly related to patients' survival [37]. Our data here showed that CXCL5 knockdown induced an increased stromal α-SMA, associated with an increased stromal Col1 while causing inhibition of PC growth and enhancing the inhibitory effect of gemcitabine on PC. Together with these studies, our data indicated the importance of accurate targeting of cancer cell-stellate cell interactions, which is a key weakness for stroma-targeting therapy.

Gemcitabine resistance in PC has been classified into intrinsic to cancer cells and extrinsic from TME [19, 38]. CXCL5 knockdown sensitized PC cell response to gemcitabine *in vitro* by directly affecting cancer cells to overcome the intrinsic resistance to gemcitabine. CXCL5 knockdown also enhanced the inhibitory effect of gemcitabine on PC growth in a mouse by either reducing the intrinsic resistance of cancer cells via decreasing proliferation and promoting apoptosis of cancer cells or modulating tumour microenvironment via regulation of its main components including Col1 and α-SMA to attenuate the extrinsic resistance to gemcitabine. These data suggested that CXCL5 mediated chemoresistance in PC via multiple signalling pathways, which was confirmed by our proteomic study using NC and CXCL5 KD cell lines.

CXCL5 KD induced up- or down-regulation of several proteins shown from a proteomic study of the global protein profile. Some of the down-regulated genes, GSTM1, GSTM3 and DPYD were discovered to be involved in drug metabolism by KEGG pathway analysis (**Figure 5D**), suggesting that CXCL5 could contribute to chemoresistance by regulation of drug metabolic pathway. GO function analysis identified a few up-regulated genes including FDX1, DPYD and FXN that affect oxidoreductase activity and iron-sulphur cluster binding, and a few down-regulated genes (GSTM1, GSTM3, RPE65 and PTGES) that affect modified amino acid binding, implicating that CXCL5 could intervene a drug metabolic pathway via regulation of enzyme activity and amino acid binding. However, the detailed functions of the majority of these proteins in pancreatic cancer are unclear. Even though some of these proteins have been found anti- or pro-pancreatic cancer effects, the overall net effect from the possible network identified is unclear. These results from the proteomic analysis provided a guideline for further study of the mechanism(s) involved in the CXCL5 effect.

In conclusion, knockdown of CXCL5 suppressed pancreatic cancer and attenuated gemcitabine resistance through affecting both cancer cells and tumour microenvironment.

Acknowledgements

The authors would like to acknowledge the Australian Government Research Training Program Scholarship and Royal Australasian College of Surgeons (RACS) Foundation of Surgery Scholarship for supporting Yi Ma. Dr Hong He is supported by the Henry Baldwin Cancer Research Trust Fund. This work is supported by Austin Medical Research Foundation grants (AMRF, He & Nikfarjam), Melbourne Medical School Department of Surgery Seeding Grants (Nikfarjam-2020, He-2021), Pancare Foundation (www.pancare.org.au) and Tour De Cure grants. Yang Yang is supported by China Postdoctoral Council (No. 20180028) and Pancare Foundation.

Disclosure of conflict of interest

None.

Address correspondence to: Dr. Hong He, Department of Surgery, University of Melbourne, Austin Health, 145 Studley Rd., Heidelberg 3084, Victoria, Australia. Tel: 613 9496 5468; Fax: 613 9458 1650; E-mail: hong.he@unimelb.edu.au

References

[1] Ryan DP, Hong TS and Bardeesy N. Pancreatic adenocarcinoma. N Engl J Med 2014; 371: 1039-1049.

[2] Siegel RL, Miller KD and Jemal A. Cancer statistics, 2017. CA Cancer J Clin 2017; 67: 7-30.

[3] Oettle H. Progress in the knowledge and treatment of advanced pancreatic cancer: from benchside to bedside. Cancer Treat Rev 2014; 40: 1039-1047.

[4] Siegel RL, Miller KD and Jemal A. Cancer statistics, 2019. CA Cancer J Clin 2019; 69: 7-34.

[5] Mollenhauer J, Roether I and Kern HF. Distribution of extracellular matrix proteins in pancreatic ductal adenocarcinoma and its influence on tumor cell proliferation in vitro. Pancreas 1987; 2: 14-24.

[6] Tian C, Clauser KR, Ohlund D, Rickelt S, Huang Y, Gupta M, Mani DR, Carr SA, Tuveson DA and Hynes RO. Proteomic analyses of ECM during pancreatic ductal adenocarcinoma progression reveal different contributions by tumor and stromal cells. Proc Natl Acad Sci U S A 2019; 116: 19609-19618.

[7] Apte MV, Pirola RC and Wilson JS. Pancreatic stellate cells: a starring role in normal and diseased pancreas. Front Physiol 2012; 3: 344.

[8] Ene-Obong A, Clear AJ, Watt J, Wang J, Fatah R, Riches JC, Marshall JF, Chin-Aleong J, Chelala C, Gribben JG, Ramsay AG and Kocher HM. Activated pancreatic stellate cells sequester CD8+ T cells to reduce their infiltration of the juxtatumoral compartment of pancreatic ductal adenocarcinoma. Gastroenterology 2013; 145: 1121-1132.

[9] Provenzano PP, Cuevas C, Chang AE, Goel VK, Von Hoff DD and Hingorani SR. Enzymatic targeting of the stroma ablates physical barriers to treatment of pancreatic ductal adenocarcinoma. Cancer Cell 2012; 21: 418-429.

[10] Whittle MC and Hingorani SR. Fibroblasts in pancreatic ductal adenocarcinoma: biological mechanisms and therapeutic targets. Gastroenterology 2019; 156: 2085-2096.

[11] Cao F, Li J, Sun H, Liu S, Cui Y and Li F. HES 1 is essential for chemoresistance induced by stellate cells and is associated with poor prognosis in pancreatic cancer. Oncol Rep 2015; 33: 1883-1889.

[12] Zhang H, Wu H, Guan J, Wang L, Ren X, Shi X, Liang Z and Liu T. Paracrine SDF-1alpha signaling mediates the effects of PSCs on GEM chemoresistance through an IL-6 autocrine loop in pancreatic cancer cells. Oncotarget 2015; 6: 3085-3097.

[13] Dang H, Wu W, Wang B, Cui C, Niu J, Chen J, Chen Z and Liu Y. CXCL5 plays a promoting role in osteosarcoma cell migration and invasion in autocrine- and paracrine-dependent manners. Oncol Res 2017; 25: 177-186.

[14] O'Hayre M, Salanga CL, Handel TM and Allen SJ. Chemokines and cancer: migration, intracellular signalling and intercellular communication in the microenvironment. Biochem J 2008; 409: 635-649.

[15] Ando Y, Ohuchida K, Otsubo Y, Kibe S, Takesue S, Abe T, Iwamoto C, Shindo K, Moriyama T, Nakata K, Miyasaka Y, Ohtsuka T, Oda Y and Nakamura M. Necroptosis in pancreatic cancer promotes cancer cell migration and invasion by release of CXCL5. PLoS One 2020; 15: e0228015.

[16] Li A, King J, Moro A, Sugi MD, Dawson DW, Kaplan J, Li G, Lu X, Strieter RM, Burdick M, Go VL, Reber HA, Eibl G and Hines OJ. Overexpression of CXCL5 is associated with poor survival in patients with pancreatic cancer. Am J Pathol 2011; 178: 1340-1349.

[17] Wang S, Wu Y, Hou Y, Guan X, Castelvetere MP, Oblak JJ, Banerjee S, Filtz TM, Sarkar FH, Chen X, Jena BP and Li C. CXCR2 macromolecular complex in pancreatic cancer: a potential therapeutic target in tumor growth. Transl Oncol 2013; 6: 216-225.

[18] Zhang R, Liu Q, Peng J, Wang M, Li T, Liu J, Cui M, Zhang X, Gao X, Liao Q and Zhao Y. CXCL5 overexpression predicts a poor prognosis in pancreatic ductal adenocarcinoma and is correlated with immune cell infiltration. J Cancer 2020; 11: 2371-2381.

[19] Binenbaum Y, Na'ara S and Gil Z. Gemcitabine resistance in pancreatic ductal adenocarcinoma. Drug Resist Updat 2015; 23: 55-68.

[20] Ahmed K, Koval A, Xu J, Bodmer A and Katanaev VL. Towards the first targeted therapy for triple-negative breast cancer: repositioning of clofazimine as a chemotherapy-compatible selective Wnt pathway inhibitor. Cancer Lett 2019; 449: 45-55.

[21] Schindelin J, Arganda-Carreras I, Frise E, Kaynig V, Longair M, Pietzsch T, Preibisch S, Rueden C, Saalfeld S, Schmid B, Tinevez JY, White DJ, Hartenstein V, Eliceiri K, Tomancak P and Cardona A. Fiji: an open-source platform for biological-image analysis. Nat Methods 2012; 9: 676-682.

[22] Tyanova S, Temu T and Cox J. The MaxQuant computational platform for mass spectrometry-based shotgun proteomics. Nat Protoc 2016; 11: 2301-2319.

[23] Tyanova S, Temu T, Sinitcyn P, Carlson A, Hein MY, Geiger T, Mann M and Cox J. The Perseus computational platform for comprehensive analysis of (prote)omics data. Nat Methods 2016; 13: 731-740.

[24] Shannon P, Markiel A, Ozier O, Baliga NS, Wang JT, Ramage D, Amin N, Schwikowski B

and Ideker T. Cytoscape: a software environment for integrated models of biomolecular interaction networks. Genome Res 2003; 13: 2498-2504.
[25] Wang K, Huynh N, Wang X, Pajic M, Parkin A, Man J, Baldwin GS, Nikfarjam M and He H. PAK inhibition by PF-3758309 enhanced the sensitivity of multiple chemotherapeutic reagents in patient-derived pancreatic cancer cell lines. Am J Transl Res 2019; 11: 3353-3364.
[26] Haber PS, Keogh GW, Apte MV, Moran CS, Stewart NL, Crawford DH, Pirola RC, McCaughan GW, Ramm GA and Wilson JS. Activation of pancreatic stellate cells in human and experimental pancreatic fibrosis. Am J Pathol 1999; 155: 1087-1095.
[27] Armstrong T, Packham G, Murphy LB, Bateman AC, Conti JA, Fine DR, Johnson CD, Benyon RC and Iredale JP. Type I collagen promotes the malignant phenotype of pancreatic ductal adenocarcinoma. Clin Cancer Res 2004; 10: 7427-7437.
[28] Egeblad M, Rasch MG and Weaver VM. Dynamic interplay between the collagen scaffold and tumor evolution. Curr Opin Cell Biol 2010; 22: 697-706.
[29] Fujita H, Ohuchida K, Mizumoto K, Egami T, Miyoshi K, Moriyama T, Cui L, Yu J, Zhao M, Manabe T and Tanaka M. Tumor-stromal interactions with direct cell contacts enhance proliferation of human pancreatic carcinoma cells. Cancer Sci 2009; 100: 2309-2317.
[30] Levental KR, Yu H, Kass L, Lakins JN, Egeblad M, Erler JT, Fong SF, Csiszar K, Giaccia A, Weninger W, Yamauchi M, Gasser DL and Weaver VM. Matrix crosslinking forces tumor progression by enhancing integrin signaling. Cell 2009; 139: 891-906.
[31] Chen Y, Kim J, Yang S, Wang H, Wu CJ, Sugimoto H, LeBleu VS and Kalluri R. Type I collagen deletion in alphaSMA(+) myofibroblasts augments immune suppression and accelerates progression of pancreatic cancer. Cancer Cell 2021; 39: 548-565, e546.
[32] Masamune A and Shimosegawa T. Pancreatic stellate cells--multi-functional cells in the pancreas. Pancreatology 2013; 13: 102-105.
[33] Haeberle L, Steiger K, Schlitter AM, Safi SA, Knoefel WT, Erkan M and Esposito I. Stromal heterogeneity in pancreatic cancer and chronic pancreatitis. Pancreatology 2018; 18: 536-549.
[34] Sinn M, Denkert C, Striefler JK, Pelzer U, Stieler JM, Bahra M, Lohneis P, Dorken B, Oettle H, Riess H and Sinn BV. alpha-Smooth muscle actin expression and desmoplastic stromal reaction in pancreatic cancer: results from the CONKO-001 study. Br J Cancer 2014; 111: 1917-1923.
[35] Ozdemir BC, Pentcheva-Hoang T, Carstens JL, Zheng X, Wu CC, Simpson TR, Laklai H, Sugimoto H, Kahlert C, Novitskiy SV, De Jesus-Acosta A, Sharma P, Heidari P, Mahmood U, Chin L, Moses HL, Weaver VM, Maitra A, Allison JP, LeBleu VS and Kalluri R. Depletion of carcinoma-associated fibroblasts and fibrosis induces immunosuppression and accelerates pancreas cancer with reduced survival. Cancer Cell 2014; 25: 719-734.
[36] Rhim AD, Oberstein PE, Thomas DH, Mirek ET, Palermo CF, Sastra SA, Dekleva EN, Saunders T, Becerra CP, Tattersall IW, Westphalen CB, Kitajewski J, Fernandez-Barrena MG, Fernandez-Zapico ME, Iacobuzio-Donahue C, Olive KP and Stanger BZ. Stromal elements act to restrain, rather than support, pancreatic ductal adenocarcinoma. Cancer Cell 2014; 25: 735-747.
[37] Wang WQ, Liu L, Xu HX, Luo GP, Chen T, Wu CT, Xu YF, Xu J, Liu C, Zhang B, Long J, Tang ZY and Yu XJ. Intratumoral alpha-SMA enhances the prognostic potency of CD34 associated with maintenance of microvessel integrity in hepatocellular carcinoma and pancreatic cancer. PLoS One 2013; 8: e71189.
[38] Zeng S, Pottler M, Lan B, Grutzmann R, Pilarsky C and Yang H. Chemoresistance in pancreatic cancer. Int J Mol Sci 2019; 20: 4504.

Supplementary Table 1. Primers used in RT-PCR

CXCL1	Forward: AACCGAAGTCATAGCCACAC
	Reverse: GTTGGATTTGTCACTGTTCAGC
CXCL2	Forward: CGAAGTCATAGCCACACTCAAG
	Reverse: CTTCTGGTCAGTTGGATTTGC
CXCL5	Forward: TCACAGAGTAGAACCTGGGTTAGAG
	Reverse: TGTGTCCCACCAGGACTAGAA
CXCL9	Forward: CCAACCAAGGGACTATCCACC
	Reverse: CCTTCACATCTGCTGAATCTGG
CXCL10	Forward: TGGCATTCAAGGAGTACCTCTC
	Reverse: GCAATGATCTCAACACGTGGAC
CXCL13	Forward: AATGAGCCTGGACTCAGAGC
	Reverse: GACCTCCAGAACACCTTGGA